

# Use of Kriging to Surrogate Finite Element Models of Bonded Double Cantilever Beams

Salvatore Sessa

*Research Fellow, Department of Structures for Engineering and Architecture, University of Naples Federico II, Naples, Italy*

Nunziante Valoroso

*Associate Professor, Department of Engineering, University of Naples Parthenope, Naples, Italy*

**ABSTRACT:** An algorithm based on kriging statistical interpolation for computing the surrogate response of a Finite Element model is presented. The interpolation model is calibrated via computation of Finite Element responses at a set of random occurrences of a material parameter. Such random generation concentrates at locations where the numerical model requires a higher amount of data to get the desired accuracy. As a model problem a standard fracture propagation test is analyzed. The proposed procedure is shown to be robust and accurate since responses obtained via a direct computation and use of the surrogate model turn out to be undistinguishable.

## 1. INTRODUCTION

We discuss a kriging-based surrogate model applied to the inverse identification of mode-I fracture parameters on a bonded Double Cantilever Beam (DCB) specimen.

Finite Element (FE) based inverse identification of fracture parameters from a DCB test has been recently assessed by Valoroso et al. (2013); the basic idea developed therein amounts to simulating the test via a numerical model depending on a set of (unknown) material parameters whose value is computed via minimization of a least-squares residual between the computed response and the experimental one. Objective of the present work is to develop a kriging-based surrogate model able to compute the response of a finite element model for the DCB depending on varying material parameters.

The theoretical basis of kriging interpolation, or Gaussian process regression, has been set up by Matheron (1973) based on the research of Krige (1951). The theory has acquired increasing popularity due to many successful applications developed mainly in spatial analysis and geostatistical

estimation, see e.g. Cressie (1993) for a complete overview on the subject. The basic idea of the method consists in predicting the value of a function at a given point as a weighted average of observed data, whose weights are defined by means of a stochastic model related to the observations cross-covariance. The main appeal of kriging interpolation consists in its capability to compute fast estimations of the function values at unknown placements regardless of the complexity of the observed data providing at the same time the estimation of a confidence interval.

The surrogate model discussed in this paper uses the responses of a set of FE simulations as the *observed data set* of the kriging interpolation. Specifically, a set of random points is generated in a suitable admissibility range of the material parameters to be identified and, at each point, a FE analysis is performed in order to get the corresponding *observed* response. The kriging model based on these *observations* allows evaluating estimations of the surrogate response and a corresponding confidence interval. A peculiar feature of the presented algorithm consists in the gener-

ation procedure of the random occurrences which is governed by the confidence interval amplitude, whereby new *observations* will cluster at those locations where the surrogate model is less precise.

It is worth emphasizing that the phase of data generation remains computationally costly since each point of the data set requires a full direct FE analysis. Nevertheless, in case of experimental test campaigns, the proposed procedure provides is expected to provide improved performances compared to the procedure presented in Valoroso et al. (2013) since specimens and protocols are usually fixed. Hence, the surrogate model should be generated only once and its redundant employment amounts to a set of linear computations, whereby it is faster than direct computations.

The outline of the paper is as follows. The test protocol and the relevant FE analysis is summarized in section 2. Section 3 describes the kriging interpolation procedure. The random generation algorithm and the calibration of the kriging model are presented in section 4; herein practical applications and numerical results are presented that show the capabilities of the procedure. Specifically, the model is employed for the computation of the response surrogate of cohesive bonding interface models presented in Fedele et al. (2012) and Valoroso et al. (2013) belonging to a Mode-I fracture test campaign. Finally, section 5 summarizes advantages and drawbacks of the proposed algorithm and future research directions.

## 2. MODE-I FRACTURE TEST AND FINITE ELEMENT ANALYSIS

The symmetric DCB test depicted in Figure 1 is the standard test employed for obtaining the mode-I fracture energy  $G_{Ic}$  of bonded assemblies. The specimen analyzed by Valoroso et al. (2013) consists of two adherends made of aluminum alloy Al 2024-T351 with length  $l = 200\text{mm}$ , width  $b = 20\text{mm}$  and thickness  $h = 8\text{mm}$ ; each adherend is connected to stainless steel load block.

Tests were carried out on an electromechanical material testing system shown in figure Figure 2 following the guidelines of standard ISO 25217 (2009); load and displacements data were recorded during the test.

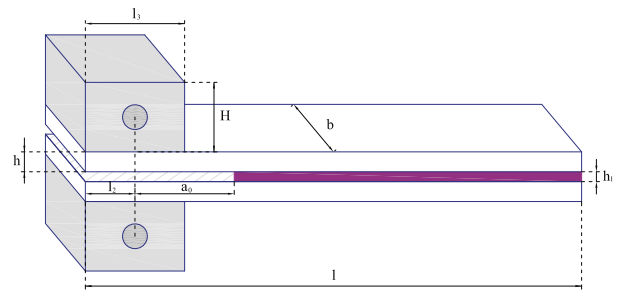


Figure 1: DCB specimen geometry.

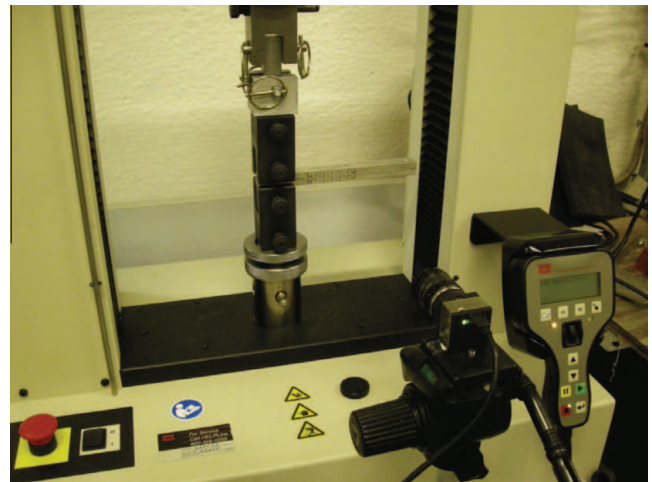


Figure 2: DCB delamination test configuration.

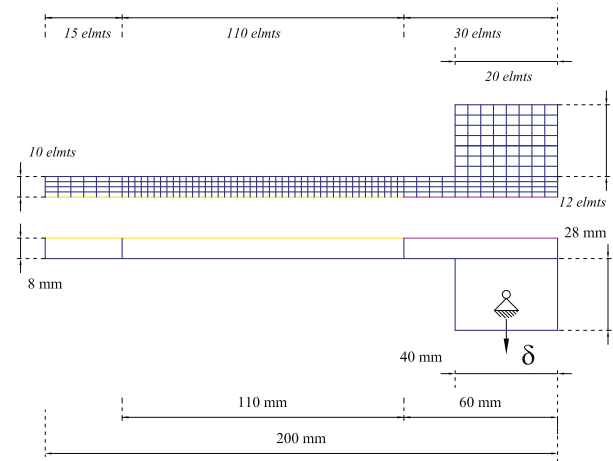


Figure 3: DCB specimen. Geometry and FE mesh used for identification.

The FE mesh used in computations is shown in Figure 3; it consists of 3580 4-node Enhanced Assumed Strain elements for the bulk material and 125 2-node interface elements. The left end of the model is free while the right part presents two sim-

ple supports at the centroids of the load blocks with an increasing vertical displacement prescribed to the upper block, see e.g. Valoroso et al. (2013) for a full detail.

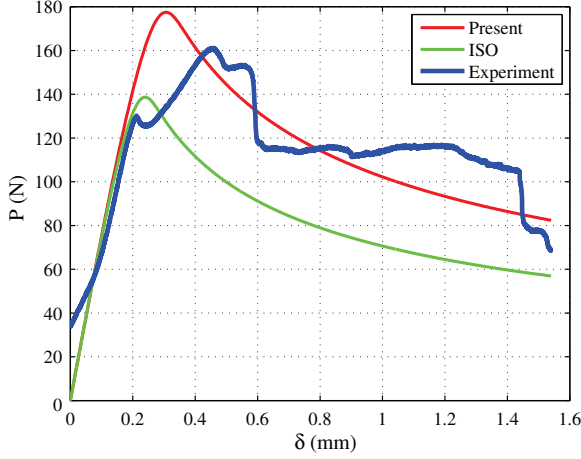


Figure 4: DCB specimen. Experimental VS computed load-deflection curves.

Measured and computed load-deflection curves are given in Figure 4. Here on the x-axis is reported the displacement  $\delta$  [mm] of the upper constraint and on the y-axis the corresponding load  $P$  [N]. The experimental load-deflection is plotted in blue; the green and the red curves are two numerical responses computed using different values of  $G_{Ic}$ , which is the target parameter of the present identification exercise.

### 3. KRIGING INTERPOLATION

Kriging interpolation performs a weighted average of the known values of a function in the neighborhood of the point of interest; it is a form of Bayesian inference of observed, or measured, data since average weights are obtained from a Gaussian regression of data. The function of interest is modeled as a Gaussian process which is defined by a *prior* normal distribution; then, a set of values associated with a spatial location is observed and the covariance of these evidences is computed. This defines, for each of the observations, a Gaussian likelihood function which is combined with the prior one in order to get an updated, *posterior* Gaussian process. The recondite action of the weighted average, concealed in the definition of the weights, consists

in computing the expected value of the posterior Gaussian process at the point of interest.

Let  $\mathbf{r} = [r_1 \dots r_n]^T$  a vector containing the  $n$  observed values of the function of interest  $R(x)$ ,  $\mathbf{x} = [x_1 \dots x_n]^T$  the vector containing their spatial location and  $\hat{x}$  the point of interest in the domain of the function  $R(x)$ . The weighted average consists in the following:

$$R(\hat{x}) \simeq \hat{r} = \mathbf{w}^T \mathbf{r} \quad (1)$$

where  $\mathbf{w}$  is the weight vector and  $\hat{r}$  the estimated value of  $R$ .

#### 3.1. Computation of the average weights

Average weights are obtained via Bayesian updating of the prior Gaussian process by inference of the cross-correlation of the observed data. From an operational point of view, it is more convenient to employ a function derived by the cross-correlation named the *variogram*, which is defined as the variance of the difference between process values at two locations ( $x_i$  and  $x_j$ ) across realizations of a stochastic process or a random field:

$$\gamma_{ij} = \gamma(|x_i - x_j|) = \text{Var} [R(x_j) - R(x_i)] \quad (2)$$

the computation of the variogram at the  $n$  observed points defines the  $(n+1) \times (n+1)$  matrix  $\mathbf{S}_d$  as:

$$\mathbf{S}_d = \begin{bmatrix} \gamma_{11} & \dots & \gamma_{1n} & 1 \\ \vdots & \ddots & \vdots & \vdots \\ \gamma_{n1} & \dots & \gamma_{nn} & 1 \\ 1 & \dots & 1 & 0 \end{bmatrix} \quad (3)$$

while the variogram at the point of interest  $\hat{x}$  defines the  $n+1$  vector  $\mathbf{s}_0$  as:

$$\mathbf{s}_0 = [\gamma(|\hat{x} - x_1|) \quad \dots \quad \gamma(|\hat{x} - x_n|) \quad 1]^T \quad (4)$$

Average weights are obtained by the combination of  $\mathbf{S}_d$  and  $\mathbf{s}_0$ :

$$\begin{bmatrix} \mathbf{w} \\ \lambda \end{bmatrix} = \mathbf{S}_d^{-1} \mathbf{s}_0 \quad (5)$$

where  $\mathbf{w}$  is the weight vector to be used in Eq. (1) and  $\lambda$  is an error parameter. Finally, the estimation of  $R(\hat{x})$  and its confidence interval amplitude  $\tau$  are:

$$R(\hat{x}) \simeq \hat{r} = \mathbf{w}^T \mathbf{r} \quad (6)$$

$$\tau = \sqrt{\frac{\mathbf{w}^T \mathbf{s}_0 + \lambda}{n}}$$

where  $n$  is the number of observations and  $\mathbf{r}$  is the vector containing the observed values.

The computation of Eq. (3) and Eq. (4) requires a proper definition of the variogram function. As long as the theoretical variogram can be computed, the described procedure is quite straightforward; nonetheless, it is frequent that the observed function is not available in mathematical form. In such circumstances approximated or empirical variograms can be used, see e.g. Cressie (1993). In the present work the Gaussian variogram has been used; it is defined as:

$$\gamma(x_i, x_j) = \begin{cases} 0; & x_i = x_j \\ c_0 + (c_s - c_0) \left( 1 - e^{-\frac{3|x_i - x_j|}{a}} \right); & x_i \neq x_j \end{cases} \quad (7)$$

where  $c_0$  is the nugget parameter, i.e. the jump of the variogram function at  $x_i - x_j = 0$ ;  $c_s$  is the sill parameter, i.e. the limit of the variogram for  $|x_i - x_j| \rightarrow \infty$  and  $a$  is the range parameter, i.e. the value of  $|x_i - x_j|$  where the difference between the variogram and its sill becomes negligible. Hereafter, the nugget parameter will be set  $c_0 = 0$  since the FEM responses are not affected by any local randomness.

#### 4. MODEL CALIBRATION ALGORITHM

The kriging interpolation procedure summarized in the previous section requires a set of observed data in order to completely define its mathematical model. While in traditional applications experimental evidences are used, in this work the observed data are defined as the responses of finite element analysis. This section presents an algorithm which aims to calibrate a kriging model for the estimation of the surrogate response of a finite element DCB test simulation.

Let then  $R^{FE}(x)$  be a response of interest computed via a finite element analysis. Such a response depends on a generic parameter  $x$  with  $x_l$  and  $x_u$  as lower and upper bound respectively. Please note that the procedure described in this section is generalized and it can be used to describe any of the responses which are usually computed by finite element analysis (such as displacements, stresses, internal forces etc). Analogously, the parameter  $x$  can

be any of the input variables of the FEM model. It is worth to emphasize that, for simplicity purposes, the presented formulation considers a single, scalar parameter only; though, an extension to multiple-parameters cases can be easily implemented but it goes beyond the aims of this work.

In order to define the set of observed data, the algorithm randomly generates occurrences of the parameter  $x$  following a Cumulative Probability Function (CDF). At the stage of the initialization of the procedure, the uniform CDF  $F_X^0(x) = (x - x_l) / (x_u - x_l)$  is considered so that a set of  $m$  occurrences of the parameter is generated and, for each one of them, the finite element analysis computes the corresponding observed value  $R^{FE}$ :

$$r_i^{FE} = R^{FE}(x_i); i = 1 \dots m \quad (8)$$

Such a set of observations  $r_i^{FE}$  and its location in the parameter space  $x_i$  are capable to define a surrogate response by kriging interpolation as long as a variogram is defined. For this purpose, the Gaussian variogram of Eq. (7) is considered; however, its parameters  $c_0$ ,  $c_s$  and  $a$  need to be conveniently calibrated taking into account the observations  $r_i^{FE}$ . This can be easily done by a minimization symplex algorithm applied to the optimization problem:

$$\begin{aligned} & [\hat{c}_0 \quad \hat{c}_s \quad \hat{a}] = \\ & = \arg \min \left[ c_0, c_s, a \left| \sum_{i=1}^m \left( r_i^{FE} - \mathbf{w}(c_0, c_s, a) \mathbf{r}_{j \neq i}^{FE} \right)^2 \right| \right] \end{aligned} \quad (9)$$

where  $r_i^{FE}$  is the  $i$ th observation and  $\mathbf{w}(c_0, c_s, a) \mathbf{r}_{j \neq i}^{FE}$  is the kriging estimate of  $r_i^{FE}$  provided by the remaining observations. In this sense, the minimizing argument is the mean square of the residual computed at each one of the observation points.

Once that the variogram is calibrated, a first-tentative surrogate model is easily defined by computing  $\mathbf{S}_q^0$ ,  $\mathbf{s}_0^0$  and  $\mathbf{w}^0$  by Eq. (3), Eq. (4) and Eq. (5) respectively, while the surrogate response at the point  $\hat{x}$  comes from Eq. (6).

The accuracy of the surrogate model depends on the number of observations  $m$  and on their distribution in the parameter domain: a larger value of  $m$  would provide better results, however, the random

generation above does not consider any information about the features of the actual response. It is convenient to perform the generation of the random locations  $x_i$  by the following recursive procedure: after the first  $m$  generations, Eq. (6) provides, for any point of the domain of  $x$ , the surrogate response and its confidence interval  $\tau(x)$  which is obviously larger where the surrogate response is less accurate. The function  $\tau(x)$  can be used as the probability density function of the random generation, if conveniently normalized. Specifically, an updated CDF can be defined as:

$$F_X^1(x) = \frac{\int_{x_l}^x \tau^0(\xi) d\xi}{\int_{x_l}^{x_u} \tau^0(\xi) d\xi} \quad (10)$$

so that the random generation will provide outcomes with higher probability where the surrogate model lacks of precision. Note that the denominator of Eq. (10) is a measure of the accuracy of the whole surrogate model since it is its cumulative error. This allows one to iterate such procedure with subsequent generations of  $m$  observation points as long as the overall error is greater than a tolerance value.

The iterative procedure for generating the surrogate model can be summarized in the following steps:

1. generation  $m$  new values of  $x_i$  with CDF  $F_X^{k-1}$ ;
2. computation of  $r_i^{FE}$  by Finite Element analysis;
3. calibration of the variogram  $\gamma^k$  and identification of the parameters  $\hat{c}_0^k$   $\hat{c}_s^k$   $\hat{a}^k$  through the optimization problem:

$$\begin{aligned} [\hat{c}_0^k \quad \hat{c}_s^k \quad \hat{a}^k] &= \arg \min [c_0, c_s, a | \\ &\left| \sum_{i=1}^{(k+1)m} \left( r_i^{FE} - \mathbf{w}(c_0, c_s, a) \mathbf{r}_{j \neq i}^{FE} \right)^2 \right| \end{aligned} \quad (11)$$

4. computation of  $\mathbf{S}_d^k$ ,  $\mathbf{s}_0^k$  and  $\mathbf{w}^k$  by Eq. (3), Eq. (4) and Eq. (5);
5. evaluation of the overall error  $\varepsilon^k = \int_{x_l}^{x_u} \tau^0(\xi) d\xi$  and convergence check;
6. updating of the CDF:

$$F_X^k(x) = \frac{\int_{x_l}^x \tau^k(\xi) d\xi}{\int_{x_l}^{x_u} \tau^k(\xi) d\xi} \quad (12)$$

while convergence is not reached, then the procedure is iterated updating  $k = k + 1$  and returning to step 1.

#### 4.1. Numerical Application

In order to provide a clearer idea about the proposed algorithm, a numerical application is presented in this section. It concerns the finite element simulation of a DCB test whose specifications are provided in Section 2, with maximum displacement of the upper load block  $\delta = 2.4mm$ . The critical fracture energy release rate  $G_{Ic}$  has been used as varying parameter  $x$  while the total energy release (i.e. the integral of the constraint reaction among the whole test) is the response of interest.

Considering the experimental results presented in Valoroso et al. (2013), the upper and lower bounds of  $G_{Ic}$  have been set to 75 and 750  $J/m^2$ . Finally, the number of generated random observations at each iteration of the algorithm has been set at  $m = 8$ . This is in order to take advantage of parallel computing: the algorithm has been implemented so that several FEM analysis run separately on different cores and a commitment of eight cores is the optimal choice for the employed hardware.

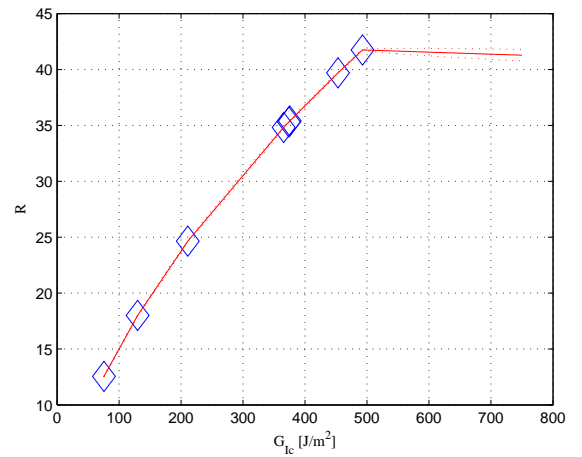


Figure 5: Surrogate response (solid line) and observations (diamonds) at the 1st iteration.

Figure 5 shows the surrogate response at the first iterations with the parameter  $G_{Ic}$  reported on the  $x$ -axis and the surrogate response  $R(G_{Ic})$  on the  $y$ -axis. The blue diamonds represent the responses computed by the FEM algorithm at each one of the

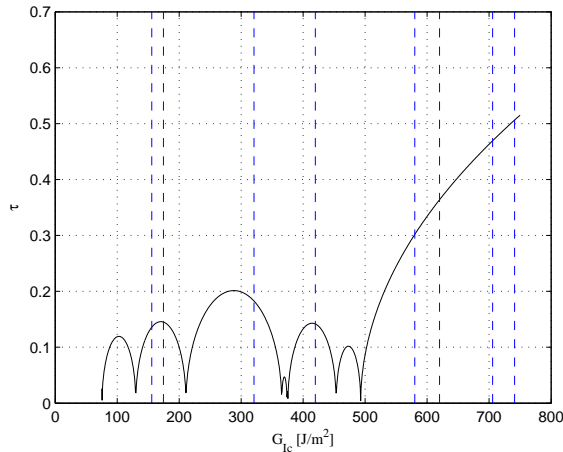


Figure 6: Normalized amplitude of the confidence interval after the 1st iteration (solid curve) and random values of the parameter generated at the 2nd iteration (blue dashed lines).

first eight randomly generated values of the parameter. The surrogate response has been subsequently computed by the kriging procedure described above and it is plotted as the red solid line. The corresponding amplitude of the confidence interval  $\tau$  is plotted as a black line in Figure 6 where the blue vertical lines correspond to the eight values of the parameter generated at iteration 2. It is worth to emphasize how the new random observations cluster where the error results higher. After five iterations (40 FEM analysis) the algorithm provides a sufficiently accurate surrogate model shown in Figure 7.

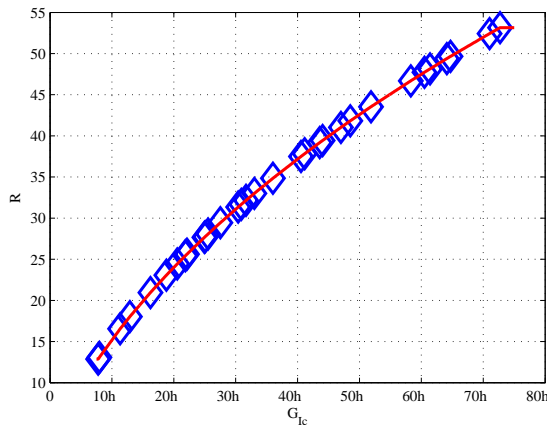


Figure 7: Surrogate response (solid line) and observations (diamonds) at the 5th iteration.

Once that the observation set corresponding to the total energy release is defined, the calibration of a kriging model can be performed for any other output of the FEM analysis.

The peculiar surrogate model has been also computed for the load–displacement response of the considered DCB specimen; specifically, each time–step of the DCB test simulation can be treated as a single, scalar response so that a kriging surrogate model can be defined. The whole set of surrogate models corresponding to each one of the responses–in–time leads to the definition of a complete load–displacement curve surrogate.

Figure 8 shows a comparison between the output of the FEM analysis (black curves) and the corresponding surrogate response (colored diamonds) for three values of the parameter  $G_{Ic}$ . A good fit of the surrogate model can easily be appreciated since the corresponding plots are not distinguishable; the maximum error of the surrogate model, for this specific case, results about 0.1%.

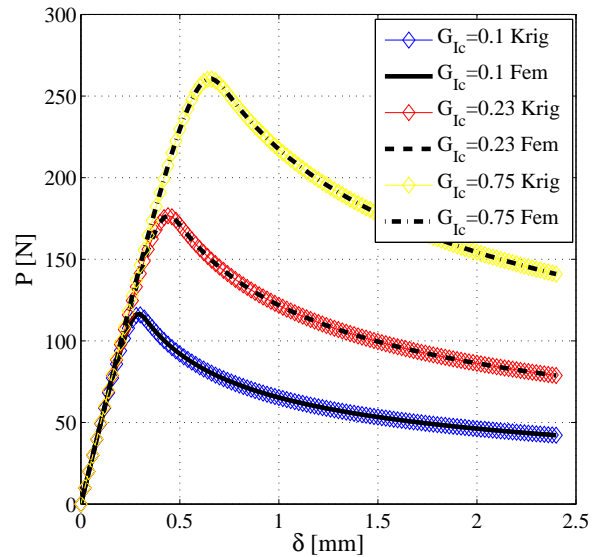


Figure 8: Comparison between surrogate responses (colored curves) and FEM analysis (black curves).

## 5. DISCUSSION AND CONCLUSIONS

A surrogate model of finite element simulations based on a kriging interpolation procedure is presented in this work. kriging interpolates observed data of a function of interest in order to predict the

function's value at an assigned point in the parameter domain. The presented procedure uses as observations the outcomes of finite element analysis performed at randomly generated values of the parameter. The peculiar capability of kriging interpolation to provide a confidence interval leads to an efficient random generation of the observations so that the generated points cluster where the surrogate model lacks of precision. The numerical application shown in Section 4.1 shows the consistency of the presented algorithm: the maximum error of the surrogate model results about 0.1% of the corresponding finite element response.

The presented algorithm is not strictly limited to applications similar to the one shown in Section 4.1. Since the procedure processes numerical responses, it is possible to perform it for any kind of numerical analysis or structural models. Even the limitation about the parameter domain can be easily overtaken: from a mathematical point of view, a convenient definition of the CDFs could generate unbounded random values of the parameter. Upper and lower bounds introduced in Section 4 are aimed at obtaining an easy implementation of the algorithm.

An interesting consideration concerns the computational times: the calibration of the kriging model required about 40 finite element analysis, thus, the pre-processing stage turns out quite computationally demanding. Although, once that the kriging model is calibrated, the presented numerical application requires about 120 sec. for a complete finite element analysis while the surrogate model runs in about 2 seconds. This enormous advantage makes such method appealing whenever several analysis are required, as in case of inverse analysis in experimental test campaigns. In general, it results convenient as long as redundant analysis are required.

The algorithm high speed is due to the fact that, once the kriging model is calibrated, the surrogate response prediction consists in linear operations with matrices and vectors. This aspect concerns a straightforward improvement of the procedure which has been omitted for lack of space. Specifically, the algorithm can be extended with a

Direct Differentiation routine in order to get the surrogate response derivatives. This is a further appealing benefit since several application cases require finite differences for the computation of their derivatives as in the case of the parameter identification presented in Valoroso et al. (2013) and concerning the same structural model employed in this work. The availability of a surrogate model providing the response derivative would permit the employment of gradient algorithm which are faster and more reliable than gradient-free algorithms. An exhaustive focus on direct differentiation would be beyond the purposes of this work but are one of the future research direction.

Further improvements concern the case of multiple parameters analysis. The procedure can be easily extended in order to be performed in a multi-dimensional parameter space; nevertheless, in this case the peculiar relationship between the parameters strongly influences the definition of the auto-correlation functions, thus, specific investigations are required. This further extension will also be a topic of the upcoming research.

## 6. REFERENCES

- Cressie, N. (1993). *Statistics for spatial data, revised edition*. John Wiley & Sons, Inc.
- Fedele, R., Sessa, S., and Valoroso, N. (2012). "Image correlation-based identification of fracture parameters for structural adhesives." *TECHNISCHE MECHANIK*, 32(2-5), 195-204.
- ISO 25217 (2009). "ISO 25217. Adhesives – Determination of the mode I fracture energy of structural adhesive joints using double cantilever beam and tapered double cantilever beam specimens." *Report no.*, Geneva, Switzerland.
- Krige, d. g. (1951). *A Statistical Approach to Some Mine Valuation and Allied Problems on the Witwatersrand*.
- Matheron, G. (1973). "The intrinsic random functions and their applications." *Advances in Applied Probability*, 5(3), pp. 439-468.
- Valoroso, N., Sessa, S., Lepore, M., and Cricri, G. (2013). "Identification of mode-i cohesive parameters for bonded interfaces based on dcb test." *Engineering Fracture Mechanics*, 104, 56-59.